Electronic Structure of the Rh-Rh Bond in $Rh_2(O_2CR)_4(PY_3)_2$ by Electron Spin Resonance Study of Their Cation Radicals

Takashi Kawamura,* Kadzuhiko Fukamachi, Takayoshi Sowa, Shigeru Hayashida, and Teijiro Yonezawa

Contribution from the Department of Hydrocarbon Chemistry, Faculty of Engineering, Kyoto University, Kyoto 606, Japan. *Received June 3, 1980*

Abstract: Electrochemical and/or radiochemical oxidations of $Rh_2(O_2CR)_4(PY_3)_2$ (R = Et, CF_3; PY_3 = PPh_3, $P(OPh)_3$, $P(OCH_2)_3CEt$) gave their cation radicals, which were studied with electron spin resonance spectroscopy. The odd-electron orbital is most reasonably assigned to the a_{1g} (in D_{4h}) orbital with Rh–Rh d_σ–d_σ bonding and Rh–P d_σ–n antibonding characters and with a larger density on the rhodium d_σ orbital. The odd-electron density on the rhodium 5s atomic orbital is less than 15% of that on the rhodium d_σ atomic orbital. The ESR results are most consistent with a single bond formulation of the Rh–Rh bond in accordance with SCF Xα-SW calculations.

Metal-metal bond lengths in tetra-μ-carboxylato-dirhodium(II) complexes are rather short (2.386–2.456 Å),[1,2] although tetra-μ-carboxylato frameworks can accommodate a pair of metal atoms with a wide variety of distances from 2.09 Å in $Mo_2(O_2CCF_3)_4$[3] to 2.72 Å in $Cu_2(O_2CH)_4(NCS)_2^{2-}$.[4] The short Rh–Rh bond was assigned some time ago as a triple bond[1,5] with an electron configuration of $\sigma^2\pi^4\delta^2\delta^{*2}\sigma_n^2\sigma_n'^2$, where σ_n and σ_n' are rhodium lone-pair orbitals expanding away from the intermetallic bonding region and consisting mainly of 5s and 5p atomic orbitals (AO).

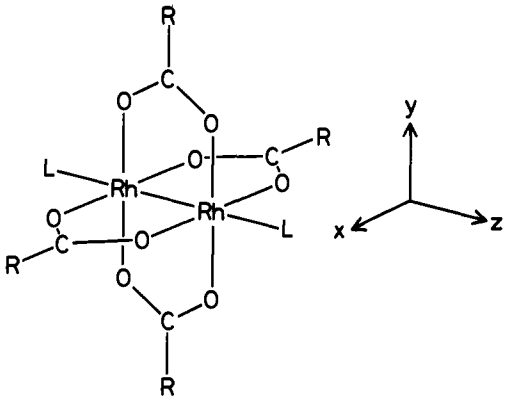

Dubicki and Martin[6] obtained a single bond configuration of $\pi^4\sigma^2\delta^2\delta^{*2}\pi^{*4}$ from SCCC–MO calculations and explained ligand dependences of electronic absorption spectra of this class of complexes along the latter bonding scheme.

Recent SCF Xα-SW calculations by Norman and his coworkers[7] gave a single bond configuration of $\sigma^2\pi^4\delta^2\pi^{*4}\delta^{*2}$ for this class of complexes. The electronic structure of the Rh–Rh bond has been explored experimentally by an ESR study of a nitroxide adduct of $Rh_2(O_2CCF_3)_4$,[8] by an analysis of the thermodynamics of adduct formations of $Rh_2(O_2CPr^n)_4$ with various bases,[9] by polarized electronic absorption spectra of a single crystal of $Rh_2(O_2CMe)_4(H_2O)_2$,[10] and by a systematic analysis of the dependence of the Rh–Rh bond length upon axial ligands,[2,11] all in favor of a single bond model or of being analyzed reasonably by relying on results of SCF Xα-SW calculations. A cation radical salt of $Rh_2(O_2CMe)_4$ has been isolated by Ziolkowski and his co-workers,[12] and its magnetic susceptibility and Rh–Rh bond length were explained with the triple bond formulation of the Rh–Rh bond.

An ESR study of an ion radical of a diamagnetic transition-metal complex may offer direct information on the shape of the HOMO or LUMO of the parent neutral molecule, thus revealing the electronic structure of the complex,[13] when all steps of the study proceed favorably.

We tried to examine anion radicals of tetra-μ-carboxylato-dirhodium(II) complexes with ESR spectra, but anions generated electrochemically[14] or radiochemically were not stable enough, if they existed. On the other hand, cation radicals of this class of complexes are stable[9,12] enough, and the odd-electron orbital of $Rh_2(O_2CEt)_4(PPh_3)_2^{+\cdot}$ was proposed to have a σ symmetry with respect to the P–Rh–Rh–P axis in a previous preliminary report.[15]

Results

Cyclic voltammograms of $Rh_2(O_2CEt)_4(PPh_3)_2$ in CH_2Cl_2 showed a quasi-reversible oxidation–reduction peak pair at $E_{1/2}$ = 0.61 V vs. standard calomel electrode (SCE) with $E_{pa} - E_{pc}$ = 70 mV and $i_{pa}/i_{pc} = 0.97 \pm 0.1$ (the potential scan rate = 60 mV/s). An integration of a current vs. time curve of the electrochemical oxidation of this complex at 0.75 V vs. SCE showed that one electron per molecule ($n = 0.9 \pm 0.2$) is transferred at this potential. An electrochemical oxidation of this complex in CH_2Cl_2 at 0.75 V vs. SCE in an ESR cavity at −20 °C gave a broad 1:2:1 triplet of 165×10^{-4} cm^{-1} at g = 2.109. When this solution was frozen and cooled to −170 °C, the spectrum changed to an axially symmetric pattern; the spectrum was reported earlier.[15] The analysis of the solid-phase spectrum was refined by comparisons with computer simulations; the refined principal values of the g and hyperfine splitting tensors are summarized

(1) Cotton, F. A.; DeBoer, B. G.; LaPrade, M. D.; Pipal, J. R.; Ucko, D. A. *J. Am. Chem. Soc.* **1970**, *92*, 2926; *Acta Crystallogr., Sect. B* **1971**, *B27*, 1664.
(2) Christoph, G. G.; Koh, Y.-B. *J. Am. Chem. Soc.* **1979**, *101*, 1422.
(3) Cotton, F. A.; Norman, J. G., Jr. *J. Coord. Chem.* **1971**, *1*, 161.
(4) Goodgame, D. M. L.; Hill, N. J.; Marsham, D. F.; Skapski, A. C.; Smart, M. L.; Troughton, P. G. H. *Chem. Commun.* **1969**, 629.
(5) Caulton, K. G.; Cotton, F. A. *J. Am. Chem. Soc.* **1971**, *93*, 1914.
(6) Dubicki, L.; Martin, R. L. *Inorg. Chem.* **1970**, *9*, 673.
(7) (a) Norman, J. G., Jr.; Kolari, H. J. *J. Am. Chem. Soc.* **1978**, *100*, 791. (b) Norman, J. G., Jr.; Renzoni, G. E.; Case, D. A. *Ibid.* **1979**, *101*, 5256.
(8) Richman, R. M.; Kuechler, T. C.; Tanner, S. P.; Drago, R. S. *J. Am. Chem. Soc.* **1977**, *99*, 1055.
(9) Drago, R. S.; Tanner, S. P.; Richman, R. M.; Long, J. R. *J. Am. Chem. Soc.* **1979**, *101*, 2897.
(10) Martin, D. S., Jr.; Webb, T. R.; Robbins, G. A.; Fanwick, P. E. *Inorg. Chem.* **1979**, *18*, 475.
(11) Koh, Y. -B.; Christoph, G. G. *Inorg. Chem.* **1979**, *18*, 1122.
(12) (a) Moszner, M.; Ziolkowsky, J. J. *Bull. Acad. Polon. Sci., Ser. Sci. Chim.* **1976**, *24*, 433. (b) Ziolkowsky, J. J.; Moszner, M.; Glowiak, T. *J. Chem. Soc., Chem. Commun.* **1977**, 760.
(13) (a) Cotton, F. A.; Pedersen, E. *J. Am. Chem. Soc.* **1975**, *97*, 303. (b) Bratt, S. W.; Symons, M. C. R. *J. Chem. Soc.*, Dalton *Trans.* **1977**, 1314. (c) Peake, B. M.; Rieger, P. H.; Robinson, B. H.; Simpson, J. *J. Am. Chem. Soc.* **1980**, *102*, 156. (d) Kawamura, T.; Hayashida, S.; Yonezawa, T. *Chem. Lett.* **1980**, 517.
(14) Das, K.; Kadish, K. M.; Bear, J. L. *Inorg. Chem.* **1978**, *17*, 930.
(15) Kawamura, T.; Fukamachi, K.; Hayashida, S. *J. Chem. Soc., Chem. Commun.* **1979**, 945.

0002-7863/81/1503-364$01.00/0

Table I. Assignments of ESR Parameters of $Rh_2(O_2CR)_4(PY_3)_2^{+\cdot}$

no.	R	PY_3	$g_\parallel$	$g_\perp$	$10^4A_\parallel$(P), cm^{-1}	$10^4A_\perp$(P), cm^{-1}	$10^4\lvert A_\parallel$(Rh)$\rvert$, cm^{-1}	$10^4\lvert A_\perp$(Rh)$\rvert$, cm^{-1}
1	Et	PPh_3	1.996	2.148	(+) 205	(+) 152	13	*a*
2	Et	$P(OPh)_3$	2.001	2.174	(+) 342	(+) 309	17	*a*
3	Et	ETPB	1.995	2.203	(+) 346	(+) 315	20 ± 2	*a*
4	CF_3	PPh_3	2.003	2.088	(+) 212	(+) 142	13.3	*a*
5	CF_3	$P(OPh)_3$	2.002	2.127	(+) 342	(+) 294	17.6	$<8^{a,b}$
6	CF_3	ETPB	2.003	2.154	(+) 373	(+) 324	20.3	$<8^{a,b}$

[a] Not resolved. [b] Estimated from the line width.

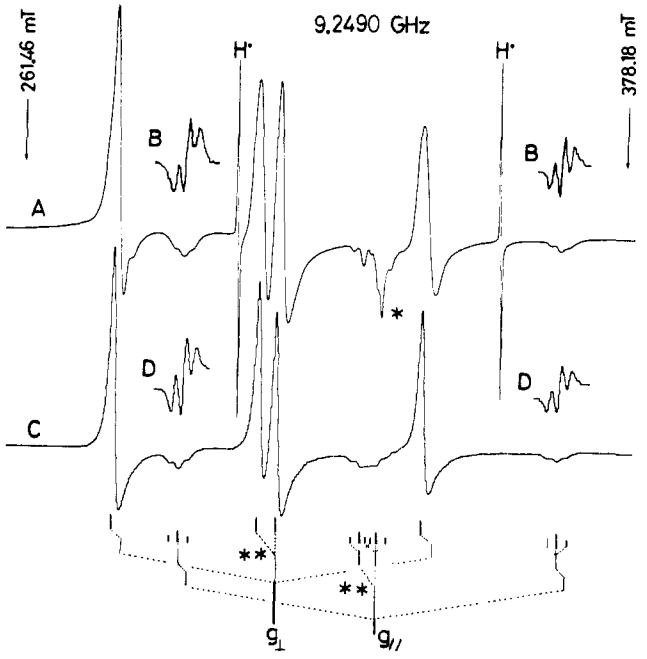

Figure 1. First (A) and second (B) derivative spectra of $Rh_2(O_2CCF_3)_4(P(OPh)_3)_2^{+\cdot}$ observed at −196 °C. The signal with the asterisk is due to unidentified species. Simulations C and D correspond to A and B, respectively. The stick spectrum at the bottom shows the analysis. The doublet splittings with the double asterisk are due to second and higher order hyperfine interactions.

in Table I (for assignments of the splitting constants, see a later section). This paramagnetic species with two pairs of magnetically equivalent $I = {}^1/_2$ nuclei (^{31}P, $I = {}^1/_2$, 100% natural abundance; ^{103}Rh, $I = {}^1/_2$, 100%) is assigned to $Rh_2(O_2CEt)_4(PPh_3)_2^{+\cdot}$ with a structure similar to that of the parent neutral molecule. The same spectrum was observed at −196 °C when a frozen solution of this complex in a 1:1 volume ratio mixture of $CFCl_3$ and CF_2BrCF_2Br (Freon mixture) was exposed to ^{60}Co γ-rays at −196 °C and annealed appropriately to decay the solvent radicals.

Electrochemical oxidations of adducts of $Rh_2(O_2CEt)_4$ with triphenylphosphite and 4-ethyl-2,6,7-trioxa-1-phosphabicyclo-[2.2.2]octane (ETPB) were chemically irreversible on cyclic voltammetry, but radiochemical oxidations of these phosphite adducts in Freon mixture solvents at −196 °C gave their cation radicals, whose ESR spectra observed at this temperature were analyzed as summarized in Table I.

Adducts of $Rh_2(O_2CCF_3)_4$ with triphenylphosphine, triphenylphosphite, and ETPB could not be electrochemically oxidized at potentials applicable to CH_2Cl_2 solutions containing tetra-*n*-butylammonium perchlorate as a supporting electrolyte. These three trifluoroacetates can be oxidized, however, to their cation radicals in Freon mixture glasses by γ irradiations. Unexpectedly, component lines were sharp in spectra of these three radicals. The spectrum of $Rh_2(O_2CCF_3)_4(P(OPh)_3)_2^{+\cdot}$ in Figure 1 was simulated well with the parameters listed in Table I and with the Lorentzian shape function of $\Delta H_{msl} = 1.1$ mT. Parameters obtained from spectra of $Rh_2(O_2CCF_3)_4(PPh_3)_2^{+\cdot}$ and $Rh_2(O_2CCF_3)_4(ETPB)_2^{+\cdot}$ are summarized also in Table I. Trial simulations gave 8×10^{-4} cm^{-1} as the upper limit of the unresolved perpendicular splitting due to a pair of nuclei of $I = {}^1/_2$ in the spectra of $Rh_2(O_2CCF_3)_4(P(OPh)_3)_2^{+\cdot}$ and $Rh_2(O_2CCF_3)_4(ETPB)_2^{+\cdot}$.

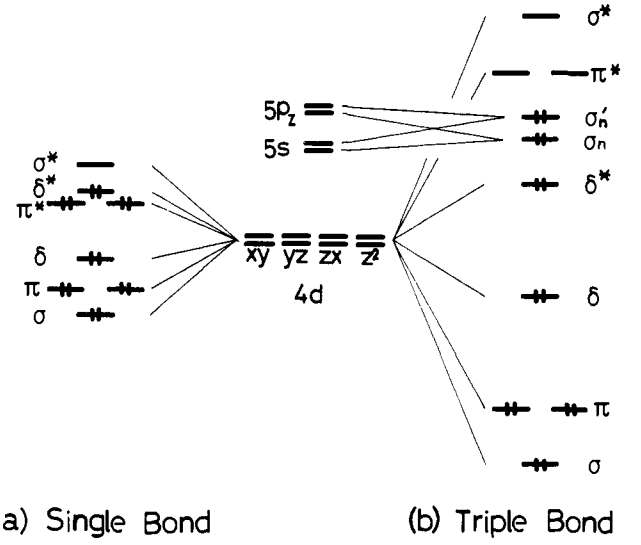

Figure 2. A schematic description of the single (a)[7] and the triple (b)[5] bond models for the Rh–Rh bond in $Rh_2(O_2CR)_4$.

Discussion

Models for Rh–Rh Bond. In both single and triple bond models, $d_{x^2-y^2}$ AOs on rhodium atoms are used to form Rh–O bonds and the remaining four 4d AOs on each rhodium atom constitute bonding and antibonding pairs of σ, π, and δ molecular orbitals (MO). In the triple bond model,[5] the interactions between 4d AOs on two rhodium atoms are described as larger than the energy difference between 4d and 5s–5p manifolds of the rhodium pair. Metallic lone-pair orbitals, σ_n and σ_n', consisting of 5s and $5p_z$ AOs are depicted as occupied MOs below π* MOs in the energy diagram, whereas π* MOs are vacant. Molecular orbital calculations[6,7] gave results in which d–d bonding interactions are not so large as the energy separation between 4d and 5s–5p manifolds and π* MOs are occupied, giving a Rh–Rh single bond formulation (Figure 2).

Spin Hamiltonian. Orbital angular momenta of electrons in the present radicals are not quenched completely as evident from appreciable shifts of some principal values of **g** tensors from the free spin value ($g_e = 2.0023$). In such cases, hyperfine tensors in a spin Hamiltonian arise not only from the first-order Fermi contact and spin dipolar coupling tensors but also from second-order terms originating from unquenched orbital angular momenta.[16] For analysis of ESR parameters of the present species, a Hamiltonian[17] given in eq 1 was treated for a doublet radical with a nondegenerate ground state according to a second-order perturbation theory:

(16) Abragam, A.; Bleaney, B. "Electron Paramagnetic Resonance of Transition Ions"; Oxford University Press: Oxford, 1970.

(17) (a) The requirement of gauge invariance was not extensively examined, but the resulting **g** tensor is practically equivalent to the gauge invariant **g** tensor.[17b] The neglect of the multicenter AO integrals is assumed implicitly in this Hamiltonian. (b) Stone, A. J. *Proc. R. Soc. London, Ser. A* **1963**, *271*, 424.

$$\mathcal{H} = g_e\beta\sum_i H\cdot s_i + \beta\sum_i\sum_k H\cdot l_{ik} + \sum_i\sum_k \zeta_k l_{ik}\cdot s_i - g_e\beta g_N\beta_N\sum_i r_{iN}^{-3}[s_i\cdot I_N - 3(n_{iN}\cdot s_i)(n_{iN}\cdot I_N)] + 2\beta g_N\beta_N\sum_i r_{iN}^{-3} l_{iN}\cdot I_N + a_N\sum_i s_i\cdot I_N \quad (1)$$

where l_{ik} is the orbital angular momentum of the ith electron around the kth atom, ζ_k is the one-electron spin–orbit coupling constant of the kth atom, r_{iN} is the distance between the ith electron and the magnetic nucleus, N, whose nuclear spin angular momentum is I_N, n_{iN} is the unit vector from the nucleus N to the ith electron, a_N is the magnitude of the Fermi contact term of the magnetic nucleus, and other notations have usual significances. The resulting spin Hamiltonian has the following form:

$$\mathcal{H}_{spin} = \beta\sum_{\alpha}^{xyz} H^\alpha g^{\alpha\alpha} S^\alpha + \sum_{\alpha}^{xyz} I_N{}^\alpha A_N{}^{\alpha\alpha} S^\alpha \quad (2)$$

$$\Delta g^{zz} = g^{zz} - g_e = 2\sum_{\lambda}^{\neq p}\langle\phi_p|\sum_k l_k{}^z|\phi_\lambda\rangle\langle\phi_\lambda|\sum_k \zeta_k l_k{}^z|\phi_p\rangle(\epsilon_p - \epsilon_\lambda)^{-1} \quad (3)$$

$$A_N{}^{zz} = a_N + g_e\beta g_N\beta_N\langle\phi_p|r_N{}^{-3}[3(n_N{}^z)^2 - 1]|\phi_p\rangle + 2g_e\beta g_N\beta_N\sum_{\lambda}^{\neq p}\langle\phi_p|\sum_k \zeta_k l_k{}^z|\phi_\lambda\rangle\langle\phi_\lambda|r_N{}^{-3} l_N{}^z|\phi_p\rangle(\epsilon_p - \epsilon_\lambda)^{-1} + i3g_e\beta g_N\beta_N\sum_{\lambda}^{\neq p}[\langle\phi_p|\sum_k \zeta_k l_k{}^x|\phi_\lambda\rangle\langle\phi_\lambda|r_N{}^{-3} n_N{}^z n_N{}^y|\phi_p\rangle - \langle\phi_p|\sum_k \zeta_k l_k{}^y|\phi_\lambda\rangle\langle\phi_\lambda|r_N{}^{-3} n_N{}^z n_N{}^x|\phi_p\rangle](\epsilon_p - \epsilon_\lambda)^{-1} \quad (4)$$

where ϕ and ϵ are the MO and its energy with the subscripts p and λ standing for the odd-electron orbital and for the other MOs, respectively. One-center AO integrals of directional cosines, $n_N{}^z$ etc., can be easily obtained with the method of equivalent operator.[16] The first two terms in eq 4 are the familiar Fermi contact and spin dipolar coupling terms; the latter term for an axially symmetric system is often abbreviated as $(-b, -b, 2b)$. The third and fourth terms are the second-order terms arising from unquenched orbital angular momenta. Principal values for xx and yy components can be obtained by the cyclic permutation of x, y, and z in eq 3 and 4.

Assignment of Splitting Constants. The triplet splitting of 165 $\times 10^{-4}$ cm^{-1} in the liquid-phase spectrum of $Rh_2(O_2CEt)_4(PPh_3)_2^{+\cdot}$ is consistent only with the assignment of splittings of 205 $\times 10^{-4}$ cm^{-1} in the parallel component and 152 $\times 10^{-4}$ cm^{-1} in the perpendicular component to the same pair of nuclei and that both splittings have the same sign. By neglecting corrections to the second-order terms in eq 4, we deduced the anisotropy of these splittings as $2|b| = 35 \times 10^{-4}$ cm^{-1}, which is even larger than the $2|b|$ value for ^{103}Rh nucleus with a unit spin density of its 4d orbital, 27.3 $\times 10^{-4}$ cm^{-1} (vide infra); the present splittings are attributed to the pair of ^{31}P nuclei. The physically meaningful choice of signs for these principal values is positive. The small splitting of 13 $\times 10^{-4}$ cm^{-1} in the parallel components is attributed to the pair of ^{103}Rh nuclei. On the basis of the similarity of ESR parameters, principal values of hyperfine splitting tensors of the other cation radicals are assigned as listed in Table I.

Constituents of Odd-Electron Orbital. The single electron l–s coupling constant for the 3p AO of phosphorus atom has a value between 97 and 152 cm^{-1},[18] which is far smaller than that for the rhodium 4d AO (Rh(II), 1200 cm^{-1}).[19] The phosphorus 3d AO is more diffuse than its 3p AO and expected to have an l–s coupling constant considerably smaller than that of the latter. By ignoring l–s couplings around phosphorus atoms and assuming that all the metal orbitals are not extensively mixed up with phosphorus orbitals, we may neglect the third and fourth terms in eq 4 in an analysis of the ^{31}P splitting tensors; odd-electron densities on phosphorus 3s and 3p (or 3d) AOs can be evaluated directly from the isotropic and anisotropic parts of the ^{31}P splittings, respectively. The observed large anisotropies of the ^{31}P splittings ($2b$(P) in Table II, $2b$(P) for ^{31}P with a unit 3p odd-electron density is 245 $\times 10^{-4}$ cm^{-1};[20] see a later section for the attribution of ^{31}P anisotropic splittings to the phosphorus 3p character) show that the odd electron orbital of $Rh_2(O_2CR)_4(PY_3)_2^{+\cdot}$ type radicals has large phosphorus components.

Table II. Odd-Electron Density on Phosphorus Atoms in $Rh_2(O_2CR)_4(PY_3)_2^{+\cdot}$

no.	R	PY_3	$10^4 a$(P), cm^{-1}	$10^4 \times (2b$(P)), cm^{-1}	ρ- (P 3s)	ρ- (P 3p_z)
1	Et	PPh_3	(+) 170	(+) 35	0.038	0.14
2	Et	$P(OPh)_3$	(+) 320	(+) 22	0.072	0.09
3	Et	ETPB	(+) 325	(+) 21	0.073	0.09
4	CF_3	PPh_3	(+) 165	(+) 47	0.037	0.19
5	CF_3	$P(OPh)_3$	(+) 310	(+) 32	0.070	0.13
6	CF_3	ETPB	(+) 340	(+) 33	0.077	0.13

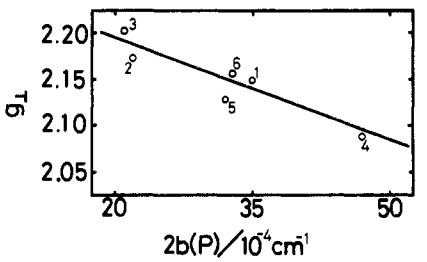

Figure 3. Correlation between ^{31}P splitting anisotropy and $g_\perp$ in $Rh_2(O_2CR)_4(PY_3)_2^{+\cdot}$. The number at each plot has the same significance as in Table I.

The maximum principal values of g tensors of the present species are larger than those of phosphorus-centered radicals (2.00–2.035)[21] and of radicals derived from carboxylic acids (2.004–2.03).[22] These results as well as the partially resolved ^{103}Rh splittings indicate that the odd-electron density on the rhodium atom, which has a large l–s coupling constant and a rather small nuclear magnetic moment, is large as well. The odd-electron orbital can be described as to be constituted from phosphorus and rhodium AOs, and the observed large shifts of $g_\perp$ from g_e are due to odd-electron densities on rhodium atoms. This picture is consistent with the observation that a decrease of the ^{31}P splitting anisotropy is accompanied by an increase of the positive shift of $g_\perp$ from g_e (Figure 3).

Unsuccessful Trial to Explain g Tensor with Triple Bond Model. The triple bond model predicts that the odd-electron orbital of $Rh_2(O_2CR)_4L_2^{+\cdot}$ would be the σ_n' (or σ_n) MO, which can be exprressed approximately as the antiphase (or in-phase) combination of 5s and 5p_z AOs on the pair of rhodium atoms (a_{2u} or a_{1g} in D_{4h}).

Since the operators l^x and l^y belong to e_g in D_{4h}, the approximate symmetry of the present radicals, an inspection of eq 3 reveals that the shift of $g_\perp$ from g_e arises from the mixing of e_u (or e_g) MOs containing rhodium 5p_x and 5p_y AOs into the a_{2u} σ_n' (or a_{1g} σ_n) odd-electron orbital through l–s couplings on rhodium atoms; doubly occupied e_u (or e_g) MOs give positive $g_\perp$ shifts and vacant e_u (or e_g) MOs negative shifts. Since rhodium 5p_x and 5p_y AOs are expected to be used mainly to form Rh–O σ bonds and are expected to remain almost vacant,[23] the $\Delta g_\perp$ value is expected to be negative contrary to the experimental observations. It is not reasonable, therefore, to assign the odd-electron orbital

(18) Malli, G.; Fraga, S. *Theor. Chim. Acta* **1966**, *7*, 80.
(19) Dunn, T. M. *Trans. Faraday Soc.* **1961**, *57*, 1440.
(20) Morton, J. R.; Preston, K. F. *J. Magn. Reson.* **1978**, *30*, 577.
(21) (a) Lyons, A. R.; Symons, M. C. R. *J. Am. Chem. Soc.* **1973**, *95*, 3483. (b) Lyons, A. R.; Symons, M. C. R. *J. Chem. Soc., Faraday Trans. 2* **1972**, *68*, 1589. (c) Kerr, C. M. L.; Webster, K.; Williams, F. *J. Phys. Chem.* **1975**, *79*, 2650.
(22) Iwasaki, M.; Eda, B.; Toriyama, K. *J. Am. Chem. Soc.* **1970**, *92*, 3212.
(23) (a) The total electron density on the three 5p AOs on a rhodium atom has been calculated to be only 0.47 for $Rh_2(O_2CH)_4(H_2O)_2^{+\cdot}$ by the SCF Xα-SW method.[19b] (b) Norman, J. G., Jr., private communication.

to the σ_n' (or σ_n) metallic lone-pair orbital.

There remains a possibility that rhodium $4d_{z^2}$, 5s, and $5p_z$ AOs mixed well together to give the highest singly occupied metallic lone-pair orbital (σ_n', a_{2u} in D_{4h}) and that the observed positive $\Delta g_\perp$ value was induced by the mixing of doubly occupied π_{RhRh} (e_u) MOs into the odd-electron orbital, σ_n', through l–s couplings in rhodium 4d AOs. However, this will be shown later to be unreasonable on the basis of the fact that the odd-electron orbital of the present radicals has σ symmetry with respect to the P–Rh–Rh–P axis and has only a few rhodium 5s and 5p characteristics.

Symmetry of Odd-Electron Orbital in Single Bond Model. In the single bond model, candidates for the odd-electron orbital are π_{RhRh}, δ_{RhRh}, π^*_{RhRh}, or δ^*_{RhRh} MO mixed with phosphorus 3d and/or σ^*_{PY} orbitals or with σ_{PY} MOs and σ_{RhRh} or σ^*_{RhRh} MO mixed with lone-pair orbitals on the pair of phosphorus atoms. If the odd-electron orbital of a present radical was a π^*_{RhRh} (or π_{RhRh}) (e_g or e_a in D_{4h}, but the D_{4h} symmetry is destroyed somehow) orbital consisting of rhodium d_{xz} and phosphorus d_{xz} or p_x orbitals, eq 3 predicts the g^{zz} (the principal value for one of the perpendicular axes for ^{31}P splittings in this model) should have a fairly large value in comparison to g^{xx} and g^{yy}, because the other π^*_{RhRh} (or π_{RhRh}) MO, consisting of rhodium d_{yz} AOs, is doubly occupied, exists in a close proximity in energy to the odd-electron orbital, and mixes into the odd-electron orbital by l^z. This model cannot give axially summetric and parallel **g** and hyperfine tensors. If we assume further that the odd electron migrates rapidly between the two π^*_{RhRh} (or π_{RhRh}) MOs, an apparent axial symmetry for ESR can be recovered but the shift of $g_\parallel$ ($=g^{zz}$) from g_e should be large and positive, contrary to the experimental results.

If we assume that the odd-electron orbital were a δ^*_{RhRh} (or δ_{RhRh}) MO (b_{1u} or b_{2g} in D_{4h}), the important MO(s) in the determination of $g_\parallel$ ($=g^{zz}$) are those with the b_{2u} (or b_{1g}) symmetry containing rhodium $d_{x^2-y^2}$ AOs with large weights. Since rhodium $d_{x^2-y^2}$ AOs are used mainly in Rh–O bonds and larger parts of these AOs are expected to stay in vacant MOs with the Rh–O σ-antibonding character, the shift of $g_\parallel$ from g_e is predicted to be negative by eq 3. This was observed in ESR spectra of $Mo_2(O_2CPr)_4^{+\cdot}$ ($g_\parallel = 1.941$)[13a] and $Re_2(O_2CPh)_4^{+\cdot}$ ($g_\parallel = 1.71$),[13a] which have electron configurations of $\sigma^2\pi^4\delta^1$ and $\sigma^2\pi^4\delta^2\delta^{*1}$, respectively. When the bridging ligand is substituted from propionate to more electronegative trifluoroacetate, the weight of rhodium $d_{x^2-y^2}$ AOs in the vacant MO(s) with σ^*_{RhO} character will increase and the energy of the vacant MO(s) will be stabilized. Thus the above-mentioned substitution would induce an increase of the negative shift of $g_\parallel$ from g_e. This expectation is contrary to the experimentally observed dependence of $g_\parallel$ on the bridging ligand. The observed $g_\parallel$ values have a small trend to increase upon the substitution of propionate with trifluoroacetate. This contradiction as well as values of $g_\parallel$ of tetrakis(μ-trifluoroacetato)-dirhodium(II) radicals, which are equal to g_e within experimental errors, are not consistent with the odd-electron orbital with the δ^*_{RhRh} (or δ_{RhRh}) character, either.

Surviving candidates for the odd-electron orbital are σ_{RhRh} and σ^*_{RhRh} MOs mixed with lone-pair orbitals on phosphorus atoms. When the odd-electron orbital is an a_{1g} (or a_{2u}) MO with the σ_{RhRh} (or σ^*_{RhRh}) constituent, eq 3 predicts that $g_\parallel$ ($=g^{zz}$) should be nearly equal to g_e since l^z can mix the a_{1g} (or a_{2u}) odd-electron orbital only with a_{2u} (or a_{1u}) MOs, which have little metal character because of the approximate D_{4h} symmetry of the present species. The shift of $g_\perp$ ($=g^{xx} = g^{yy}$) from g_e is predicted to be positive by eq 3 for these σ-type odd-electron orbitals because of high-lying[7] doubly occupied e_g π^*_{RhRh} (or e_u π_{RhRh}) MOs; l^x and l^y (e_g in D_{4h}) mix the a_{1g} (or a_{2u}) odd-electron orbital with e_g (or e_u) MOs. Doubly occupied π^*_{RhRh} MOs correspond to the single bond model.

If the odd-electron orbital is the a_{1g} MO consisting of σ_{RhRh} and the a_{1g} symmetry orbital of phosphorus lone-pair orbitals (n_P) and if the n_P orbital is assumed to be lying slightly below the energy level of the σ_{RhRh} MO of the hypothetical tetra-μ-carboxylato-dirhodium(II) without axial ligands, an increase of the odd-electron density on phosphorus atoms is predicted for the substitution of the axial ligand from a phosphite to the more σ-donating phosphine and for the substitution of the bridging ligand from propionate to more electronegative trifluoroacetate (see Scheme I); both of these substitutions induce a decrease of the energy difference between the n_P and σ_{RhRh} orbitals and, therefore, more mixing of these two component orbitals. This prediction is consistent with the experimental dependence of $2b(P)$ on the ligands summarized in Table II.

Scheme I

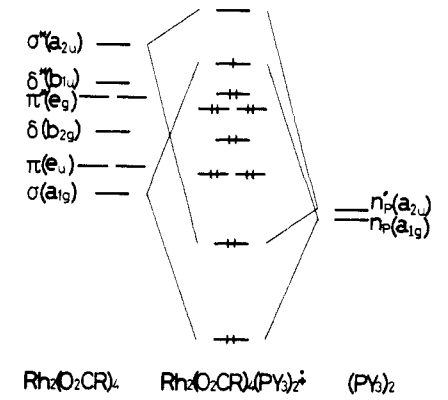

Scheme II

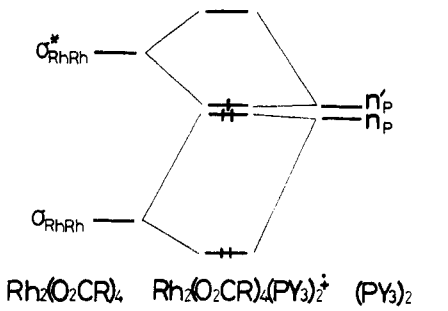

The odd-electron orbital can be an a_{2u} MO consisting of σ^*_{RhRh} and the a_{2u} combination of phosphorus lone-pair orbitals (n_P'). This model requires the in-phase combination of the zeroth order σ^*_{RhRh} and n_P' orbitals to lie, in an energy diagram, above the MO of the antiphase combination of the σ_{RhRh} orbital and the n_P lone-pair orbital, although the energy difference between the n_P and n_P' orbitals would be quite small (see Scheme II). This requirement is expected not to be satisfied, since the odd electron is distributed among rhodium and phosphorus orbitals, namely, the σ interaction between rhodium and phosphorus atoms is relatively large. Based on these considerations, we assign the odd-electron orbital to the a_{1g} MO consisting of σ_{RhRh} and n_P orbitals. This assignment is consistent with SCF Xα-SW calculations; negative values of ionization potentials of the phosphine and phosphites (PPh_3, 7.78;[24] $P(OMe)_3$, 9.25 eV[25]) are similar to the orbital energy (–8.18 eV[7a]) of σ_{RhRh} ($5a_{1g}$) of $Rh_2(O_2CH)_4$ rather than that of σ^*_{RhRh} ($4a_{2u}$, –4.78 eV[7a]).

Odd-Electron Distribution. Phosphorus atoms offer s–p hybrid lone-pair orbitals to the odd-electron orbital. Odd-electron densities on them can be evaluated by dividing isotropic and anisotropic parts of ^{31}P splittings by the corresponding theoretical splittings of this nucleus with the unit 3s and 3p odd-electron densities,[20,26] if we neglect the inner-shell spin polarization on phosphorus atoms. Thus the evaluated densities are listed in Table II.

(24) Debies, T. P.; Rabalais, J. W. *Inorg. Chem.* **1974**, *13*, 308.
(25) Betteridge, D.; Thompson, M.; Baker, A. D.; Kemp, N. R. *Anal. Chem.* **1972**, 44, 2005.
(26) The present neglect of the third and fourth terms of eq 4 may have given a systematic error of the order of $\rho(P\ p_z)^{1/2} \times$ (weight of phosphorus 3p AOs in the π_{RhRh} or π^*_{RhRh} MO)$^{1/2} \times \Delta g_\perp$ to the estimated value of $\rho(P\ p_z)$ at maximum.

Table III. Probable Range of Odd-Electron Density on Rh Atoms in $Rh_2(O_2CCF_3)_4(PY_3)_2^{+\cdot}$

PY_3	method	$10^4a \times$ (Rh), cm^{-1}	$10^4 \times$ (2b(Rh)), cm^{-1}	ρ- (Rh 5s)	ρ- (Rh $4d_{z^2}$)
$P(OPh)_3$	Rh(0)[a]	(−) 10-14	(−) 9-14	~0.05	0.3-0.6
$P(OPh)_3$	Rh(II)[b]	(−) 9-4	(−) 9-14	0.02-0.03	0.3-0.6
ETPB	Rh(0)[a]	(−) 10-5	(−) 11-16	~0.06	0.4-0.7
ETPB	Rh(II)[b]	(−) 10-4	(−) 11-16	~0.03	0.4-0.6

[a] With use of the atomic parameters, Q^V(Rh) and 2B(Rh), for Rh(0). [b] With use of the atomic parameters for Rh(II).

A probable range of the odd-electron density on the rhodium atom can be estimated for $Rh_2(O_2CCF_3)_4(P(OPh)_3)_2^{+\cdot}$ and $Rh_2(O_2CCF_3)_4(ETPB)_2^{+\cdot}$ from their resolved ^{103}Rh parallel splittings and estimated upper limits of perpendicular splittings. With the assumption that π^*_{RhRh} orbitals are localized on the Rh–Rh bond and that the odd-electron orbital is the a_{1g} orbital consisting of the σ_{RhRh} orbital according to the foregoing analysis, eq 3 and 4 correlate the ^{103}Rh splittings to the odd-electron densities on Rh $4d_{z^2}$ and 5s AOs, ρ(Rh d_{z^2}) and ρ(Rh s), as

$$A_{\parallel}(\mathrm{Rh}) = a(\mathrm{Rh}) + 2B(\mathrm{Rh})\rho(\mathrm{Rh}\ d_{z^2}) - (1/4)B(\mathrm{Rh})\Delta g_{\perp} \quad (5)$$

$$A_{\perp}(\mathrm{Rh}) = a(\mathrm{Rh}) - B(\mathrm{Rh})\rho(\mathrm{Rh}\ d_{z^2}) + (15/8)B(\mathrm{Rh})\Delta g_{\perp} \quad (6)$$

where 2B(Rh) is the spin dipolar splitting of ^{103}Rh with the unit odd-electron density on its $4d_{z^2}$ orbital. The Fermi contact term, a(Rh), can be given as the sum of the inner-shell spin polarization term proportional to ρ(Rh d_{z^2}) and the term due to the 5s odd-electron density:

$$a(\mathrm{Rh}) = Q^1(\mathrm{Rh})\rho(\mathrm{Rh}\ d_{z^2}) + Q^V(\mathrm{Rh})\rho(\mathrm{Rh\ s}) \quad (7)$$

Meaningful odd-electron densities on rhodium atoms can be obtained only by assuming negative signs for $A_{\parallel}$(Rh) and $A_{\perp}$(Rh). The value of 32.1×10^{-4} cm^{-1} has been proposed for the inner-shell polarization constant, Q^1(Rh).[27] The atomic parameters, Q^V(Rh) and 2B(Rh), were calculated to be -789×10^{-4} and -27.3×10^{-4} cm^{-1},[28] respectively, from AOs of Rh(II) with the electron configuration of $(4d)^6(5s)^1$ obtained by the method of Herman and Skillman[29] followed by relativistic corrections for Q^V(Rh) proposed by Mackey and Wood.[20,30] Although the formula charge of rhodium atoms in the present radicals is 2.5+, its net charge would be even less than 2+.[7b] Therefore, Q^V(Rh) and 2B(Rh) values for Rh(II) and Rh(0)[20] are used to estimate probable ranges of the odd-electron densities on the rhodium atoms (Table III).[31]

The contribution of the $5p_z$ character to the ^{103}Rh spin dipolar coupling has been ignored in the present analysis. However, this omission is not important in the estimation of the $4d_{z^2}$ odd-electron density, because $\langle r^{-3} \rangle$, which is proportional to 2B(Rh), should be considerably smaller for the 5p AO than that for the 4d AO. The sum of the odd-electron densities on the $4d_{z^2}$ and 5s AOs on both of the rhodium atoms is estimated already as larger than 0.66 (Table III), therefore, the $5p_z$ odd-electron density is expected to be small. Since the 5p AO is lying higher in energy than the 5s AO, the $5p_z$ odd-electron density is not likely to be much larger than the 5s odd-electron density; the latter was estimated to be less than 15% of that on the $4d_{z^2}$ AO. Thus we conclude that the odd-electron orbital is not a metallic lone pair, σ_n or σ_n', consisting of 5s and $5p_z$ AOs with an appreciable contribution of $4d_{z^2}$ AOs but the d_{z^2}–d_{z^2} intermetallic σ orbital contaminated with 5s and probably $5p_z$ AOs.

Concluding Remarks

The highest occupied orbital is most reasonably assigned to the a_{1g} (in D_{4h}) orbital consisting mainly of phosphorus lone-pair and rhodium intermetallic d_σ orbitals with a larger weight for the latter orbital. This orbital has Rh–Rh d_σ–d_σ bonding and Rh–P σ-antibonding characteristics and corresponds to the $8a_g$ MO of $Rh_2(O_2CH)_4(H_2O)_2$ calculated with the SCF Xα-SW method by Norman and Kolari.[7a] The $8a_g$ MO is reported to be consisting of 57% rhodium (42% $4d_{z^2}$, 9% 5s, and 6% $5p_z$) and 28% water components,[7a,23b] which is not very different from the present results. Thus, the present ESR results can be rationalized most reasonably with the single bond model for the Rh–Rh bond, in which the metallic lone-pair orbitals are absent in the occupied MOs.[32]

The energy level of the σ_{RhRh} MO of the hypothetical $Rh_2(O_2CR)_4$, R = Et and CF_3, without axial ligands is estimated to be higher than those of lone-pair orbitals of triphenylphosphine (−7.8 eV)[24] and phosphites ($P(OMe)_3$, −9.3 eV)[25] more or less in parallel to SCF Xα-SW calculations (the energy level of the σ_{RhRh} MO, $5a_{1g}$, of $Rh_2(O_2CH)_4$ was −8.18 eV).[7a] Upon interaction with phosphorus lone-pair orbitals, the σ_{RhRh} MO with Rh–P σ-antibonding character shifted upward jumping π_{RhRh}, δ_{RhRh}, π^*_{RhRh}, and δ^*_{RhRh} MOs, which have been calculated to have higher orbital energies than the σ_{RhRh} MO in $Rh_2(O_2CH)_4$,[7] to the highest occupied level, suggesting that π- and δ-type intermetallic interactions are weak in comparison to the Rh–P σ interaction. The π- and δ-type MOs may have shifted downward more or less by interacting with vacant orbitals on phosphorus atoms, but these downward shifts are expected to be rather small because the bond length between the rhodium atom and the axial ligand in this class of neutral complexes has been accepted as rather longer than normal.[1,2,7,33]

The lone-pair orbital on the phosphorus atom interacts considerably with the rhodium d_σ orbital, perturbing the intermetallic σ bond. A similar bonding scheme was deduced for the cobalt-phosphorus bond in $Co_2(CO)_6(Pn\text{-}Bu_3)_2^{-\cdot}$ with a D_{3d} geometry by an ESR study.[13d] The orbital interaction scheme in a previous section consistent with the ESR results is in accordance with the analysis that the trans effect of the axial ligand on the Rh–Rh bond arises from interactions between σ lone pairs on the axial ligands and σ_{RhRh} and σ^*_{RhRh} MOs.[7] The odd-electron densities on phosphorus atoms of phosphite adduct radicals are smaller than those of phosphine adducts, corresponding to the fact phosphites are weaker σ perturbers than phosphine. The σ trans effect theory thus predicts shorter Rh–Rh lengths in phosphite adducts; the Rh–Rh length in $Rh_2(O_2CMe)_4(P(OPh)_3)_2$ is 2.443 Å which is 0.006 Å shorter than that in $Rh_2(O_2CMe)_4(PPh_3)_2$.[33]

Note Added in Proof. Our recent ab initio HF calculation on neutral $Rh_2(O_2CH)_4(PH_3)_2$ gives a HOMO with the σ_{RhRh} and σ^*_{RhP} characteristics in accordance with results reported here but with smaller phosphorus lone pair components and considerably greater rhodium $5p_z$ components (H. Nakatsuji, J. Ushio, K. Kanda, Y. Onishi, T. Kawamura, and T. Yonezawa, to be submitted). A recent SCF Xα-SW treatment of the same molecule by Burnsten and Cotton (F. A. Cotton, private communication) also gives a HOMO with the σ_{RhRh} and σ^*_{RhP} characteristics but with substantially greater phosphorus components.

Experimental Section

Materials. Ethanol adducts of tetrakis(μ-trifluoroacetato)-dirhodium(II) and tetrakis(μ-trifluoroacetato)-dirhodium(II) were prepared by known methods.[34] The phosphine or phosphite dissolved in methanol or ether was added to a cold methanol solution of an ethanol adduct of tetra-μ-carboxylato-dirhodium(II) in a mole ratio of 2:1 under

(27) Muniz, R. P. A.; Vugman, N. V.; Danon, J. *J. Chem. Phys.* **1971**, *54*, 1284.

(28) Note that g_N is negative for ^{103}Rh.

(29) Herman, F.; Skillman, S. "Atomic Structure Calculations"; Prentice-Hall: Englewood Cliffs, NJ, 1963.

(30) Mackey, J. H.; Wood, D. E. *J. Chem. Phys.* **1970**, *52*, 4914.

(31) Because of the assumption of the localized π^*_{RhRh} MO, the third terms in eq 5 and 6 could have been over corrections due to the unquenched orbital angular momenta of the electrons, which could have resulted in an overestimation of ρ(Rh d_{z^2}) to the extent of ρ(P p_z)$^{1/2}$ × (weight of 3p AOs of a phosphorus atom in the π^*_{RhRh} MO)$^{1/2}$ × $\Delta g_{\perp}$.

(32) The absence of metallic lone-pair orbitals consisting of $(n+1)$s and $(n+1)$p AOs in the occupied MOs has been proved by ESR studies of $Re_2(O_2CPh)_4^{+\cdot}$ and $Tc_2Cl_8^{3-\cdot}$,[13a] which have the electron configuration of a metal–metal quadruple bond with an extra electron.

(33) Christoph, G. G.; Halpern, J.; Khare, G. P.; Koh. Y. -B., private communication.

(34) (a) Rempel, G. A.; Legzdins, P.; Smith, H.; Wilkinson, G.; Ucko, D. A. *Inorg. Synth.* **1972**, *13*, 90. (b) Winkhaus, G.; Ziegler, P. *Z. Anorg. Allg. Chem.* **1967**, *350*, 51.

the atmosphere of argon. The immediately precipitated orange to dark brown crystals were collected and washed with methanol and ether. The propionates were recrystalized from cyclohexane. The trifluoroacetates were used without futher purification.

Electrochemistry. Cyclic voltammetry studies were conducted by using a Hokuto-Denko HB-107A function generator and a HB-104A potentiostat/galvanostat and recorded on a Hitachi 057-1001 X-Y recorder. The electrolysis for ESR measurements and coulometry were performed with a home-made potentiostat, and the current was monitored on a Rikadenki B-161 recorder. The electrolyte solution was CH_2Cl_2 containing n-Bu_4NClO_4 as a supporting electrolyte and 0.1–1 mmol/L of a rhodium complex. Working and auxiliary electrodes were Pt wires for cyclic voltammetry experiments and Au wires for studies of coulometry and electrolysis for ESR. Electrolysis ESR studies were performed with an Allendoerfer type cell with a helix-working electrode[35] and a Maki-Geske type cell.[36]

ESR Spectra. These were obtained on a JEOL PE-2X spectrometer modified with a JEOL ES-SCXA gunn diode microwave unit by using a JES-VT-3A temperature controller or a JES-UCD-2X liquid-nitrogen Dewar bottle. The field sweep was monitored by proton NMR. NMR radio and ESR microwave frequencies were counted on a Takedariken TR-5501 frequency counter equipped with a TR-5023 frequency converter.

Irradiations. Deoxygenated Freon mixture solutions of a rhodium complex were frozen glassily at −196 °C and exposed to ^{60}Co γ-rays at this temperature at a dose rate of 0.04 Mrad/h for up to 40 h. Irradiated samples were annealed at temperatures between −170 to −100 °C in a cold nitrogen gas flow by using a JEOL JES-VT-3A temperature controller.

Simulation of Spectra. Two types of Fortran programs were prepared for simulation of ESR spectra of randomly oriented radicals with an axially symmetric spin Hamiltonian containing quadrupolar couplings. Quadrupolar couplings were included for general application purposes, although these couplings are not applicable to the present radicals. The first program is based on a second-order perturbation solution[37] of the Hamiltonian and takes only the allowed transitions into account. The second program calculates a stick spectrum due to the allowed transitions and the forbidden ones with nonnegligible transition probabilities (threshold, 5%, for example) originating from manually selected nuclei (with large hyperfine couplings and/or quadrupolar couplings) by careful interpolations of eigenvalues and transition moments obtained by solving secular equations for the corresponding spin Hamiltonian at three or four selected magnetic fields. Further splittings due to the remaining nuclei with small hyperfine couplings were treated with a second-order perturbation method. A stick spectrum thus obtained at a given orientation was artificially broadened by an appropriate Gaussian or Lorentzian shape function. Spectra calculated at orientations with an angle increment of 0.5–2° were added together to give a simulated spectrum for randomly oriented radicals. A typical CPU time to calculate a spectrum of a present radical was less than 1 s by the first program and 1–2 s by the second program on a FACOM M200 computer.

Experimental spectra were analyzed by trial-and-error comparisons with simulation spectra calculated with the first program and finally with the second program. The improvement of analyses by the second program was only minor for the present species.

Acknowledgment. We wish to thank Professor G. G. Christoph (Columbus, OH) for supplying X-ray structures of $Rh_2(O_2CMe)_4(PPh_3)_2$ and $Rh_2(O_2CMe)_4(P(OPh)_3)_2$ before publication. We also express our appreciation to Professor J. G. Norman, Jr. (Seattle, WA), for supplying detailed MOs obtained with SCF Xα-SW calculations. We are indebted to Dr. C. Satoko (Okazaki, Japan) for calculations of the Hartree–Fock–Slater AOs of Rh(II) on a HITAC M200 computer at the Institute of Molecular Science. We are grateful to Professor K. Okamoto and Dr. K. Komatsu (Kyoto, Japan) for cyclic voltammetry instruments. Simulations of ESR spectra were performed on a FACOM M200 computer at the Data Processing Center of Kyoto University. Samples were exposed to γ-rays at the Research Laboratory of Radioisotopes of Kyoto University.

(35) Allendoerfer, R. D.; Martinchek, G. A.; Bruckenstein, S. *Anal. Chem.* **1975**, *47*, 890.
(36) Maki, A. H.; Geske, D. H. *J. Am. Chem. Soc.* **1961**, *83*, 1852.
(37) Bleaney, B. *Philos. Mag.* **1951**, *42*, 441.

Mechanism of the Formation of Dihydrogen from the Photoinduced Reactions of Poly(pyridine)ruthenium(II) and Poly(pyridine)rhodium(III) Complexes

S.-F. Chan, Mei Chou, Carol Creutz,* Tadashi Matsubara, and Norman Sutin*

Contribution from the Chemistry Department, Brookhaven National Laboratory, Upton, New York 11973. *Received May 16, 1980*

Abstract: The irradiation of $Ru(bpy)_3^{2+}$, $Rh(bpy)_3^{3+}$, and triethanolamine (TEOA) solutions 10^9 8, 25 °C) with 450 ± 20-nm light yields rhodium(I) ($\Phi = 0.13 \pm 0.02$) (units for Φ in mol einstein^{-1} throughout the paper) and dihydrogen ($\Phi = 0.11 \pm 0.02$) in the absence and presence of platinum, respectively. A detailed mechanistic scheme has been deduced from the results of continuous- and flash-photolysis experiments: light absorption by $Ru(bpy)_3^{2+}$ gives the excited state $*Ru(bpy)_3^{2+}$ which is oxidized by $Rh(bpy)_3^{3+}$ ($k = 3.9 \times 10^8$ M^{-1} s^{-1}) yielding $Ru(bpy)_3^{3+}$ and $Rh(bpy)_3^{2+}$ with a cage escape yield of 0.15 ± 0.03. Back-reaction of $Ru(bpy)_3^{3+}$ with $Rh(bpy)_3^{2+}$ ($k = 3 \times 10^9$ M^{-1} s^{-1}) is prevented by reduction of $Ru(bpy)_3^{3+}$ by TEOA ($k = 0.2 \times 10^8$ M^{-1} s^{-1}). The oxidized TEOA radical so generated undergoes a TEOA-promoted rearrangement ($k = 0.3 \times 10^7$ M^{-1} s^{-1}) to a reducing radical. The latter reduces $Rh(bpy)_3^{2+}$ so that the net yield for $Rh(bpy)_3^{2+}$ formation is 0.3 ± 0.1. Rate-determining loss of bpy from $Rh(bpy)_3^{2+}$ ($k = 1.0 \pm 0.5$ s^{-1}) is followed by rapid reduction of $Rh(bpy)_2^{2+}$ by $Rh(bpy)_3^{2+}$ ($k = 0.3 \times 10^9$ M^{-1} s^{-1}) giving $Rh(bpy)_3^{3+}$ and Rh(I). In the presence of platinum, H_2 is formed at the expense of Rh(I); catalyzed reaction of Rh(II) with water occurs before disproportionation to Rh(I) can take place. The H_2 quantum yield in this system is limited only by the cage escape of the primary products, the homogeneous and heterogeneous "dark reactions" being very efficient. In the course of this study the electrochemistry of $Rh(bpy)_3^{3+}$, $Rh(phen)_3^{3+}$, and $Rh(bpy)_2(OH)_2^+$ in aqueous solution was investigated, and the quenching of $Ru(bpy)_3^{2+}$ emission by these Rh(III) complexes was characterized.

Introduction

Tris(2,2′-bipyridine)ruthenium(II)[1] ($Ru(bpy)_3^{2+}$) has now proved a useful mediator in the photoreduction of water[2] in both heterogeneous[3-9] and homogeneous systems.[10] For several of the heterogeneous systems studied so far, the following sequence of

(1) For recent reviews see: Sutin, N.; Creutz, C. *Adv. Chem. Ser.* **1978**, *No. 168*, 1; Sutin, N. *J. Photochem.* **1979**, *10*, 19; Whitten, D. G. *Acc. Chem. Res.* **1980**, *13*, 83.
(2) Sutin, N.; Creutz, C. *Pure Appl. Chem.*, in press.
(3) Kalyanasundaram, K.; Kiwi, J.; Grätzel, M. *Helv. Chim. Acta* **1978**, *61*, 2720.

0002-7863/81/1503-369$01.00/0